StO_2 maps (lower) of the esophagus tissue (i) before the stomach removal, (ii) after the stomach removal, (iii) two minutes after the KCl injection, (iv) four minutes after the KCl injection and (v) twenty minutes after the KCl injection.
doi:10.1371/journal.pone.0099055.g004

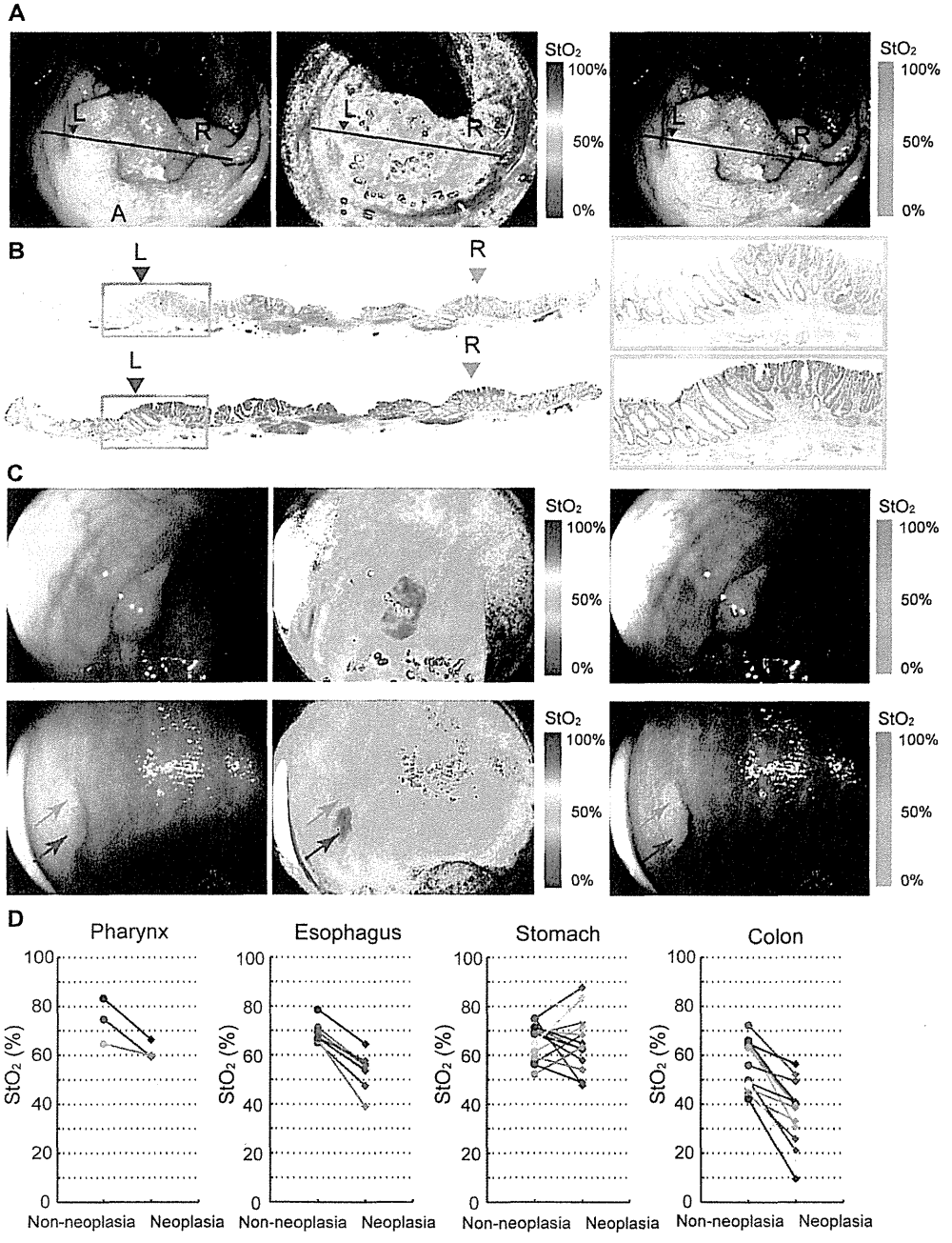

Figure 5. StO_2 maps obtained in human subject research. (A) White light image by endoscopic observation in rectal adenocarcinoma (left). Line (L-R) corresponds to cross-section of pathological diagnosis. StO_2 map visualized by laser endoscope system (middle: pseudocolor StO_2 image; right: StO_2 overlay image). (B) Cross-section appearance stained with H&E (upper) and HIF1 alpha antibody (lower) corresponding to the hypoxic area visualized with StO_2 map. (C) Endoscopic images of a colorectal adenoma (upper) showing clear hypoxia: white light image (upper left), pseudocolor StO_2 map (upper middle) and overlayed image (upper right). Another case of a colonic lesion (lower) consisting of an adenoma (red arrow) and a hyperplasia (blue arrow): white light image (lower left), pseudocolor StO_2 map (lower middle) and overlayed image (lower right). Only the adenoma was detected as hypoxia. (D) Observed StO_2 differences between neoplastic and non-neoplastic areas: For comparing pathology specimens and endoscope images, the line on the endoscopic image corresponding to the cross-section was determined. StO_2 levels at neoplasic and non-neoplasic areas along this line were then calculated using this StO_2 map.
doi:10.1371/journal.pone.0099055.g005

Table 1. Patients Characteristics.

(n = 40)	
Age	
Mean (y)	70.8
Range (y)	49–85
Gender n (%)	
Male	32 (80%)
Female	8 (20%)
Location n (%)	
Pharynx	3 (7%)
Esophagus	8 (20%)
Stomach	15 (38%)
Colorectum	14 (35%)

doi:10.1371/journal.pone.0099055.t001

clinicopathological findings between hypoxic cases and non-hypoxic including hyperoxic cases (Table 2). Further examination of organ specific hypoxia will be required.

Our endoscopic hypoxia imaging method provides a better opportunity to investigate the characteristics of cancer hypoxia. Some techniques detecting hypoxia by capillary methods, molecular biologic analysis and immunohistochemistry using histologic specimens have been reported. In the capillary method and molecular biological analysis [19], hypoxic conditions can be observed in only limited parts of the whole tumor, and features of whole tumors with hypoxia cannot be visualized. On immunohistochemistry using histologic specimens, visualization in real time is impossible. However, hypoxia imaging using this system is superior in visualizing the hypoxic conditions of whole tumors both sequentially and in real-time. No other method can simultaneously monitor oxygen concentrations in both cancerous and noncancerous areas.

Table 2. Clinicopathological findings of the study with gastric cancer patients.

		Hypoxia (n = 9)	Non-hypoxia (n = 6)
Age (y)	≥ 70 (n = 9)	5 (56%)	4 (44%)
	<70 (n = 6)	4 (67%)	2 (33%)
Gender	Male (n = 11)	6 (55%)	5 (45%)
	Female (n = 4)	3 (75%)	1 (25%)
Histologic type	Dif. (n = 12)	7 (58%)	5 (42%)
	Undif. (n = 3)	2 (67%)	1 (33%)
Macroscopic type	Elevated (n = 4)	3 (75%)	1 (25%)
	Depressed (n = 11)	6 (55%)	5 (45%)
Size (cm)	≥ 2 (n = 7)	5 (71%)	2 (29%)
	<2 (n = 8)	4 (50%)	4 (50%)
Location	U (n = 1)	1 (100%)	0 (0%)
	M (n = 10)	5 (50%)	5 (50%)
	L (n = 4)	3 (75%)	1 (25%)

doi:10.1371/journal.pone.0099055.t002

Our data strongly suggest that the microenvironment of oxygen supply to the tumor is spatially and temporally heterogeneous. This endoscope system enables us to observe spatial and temporal information of hypoxic conditions in human tumors. Moreover, we can directly acquire human cancer cells under various hypoxic conditions from biopsy samples. From these features, this endoscope system is expected to contribute to research into cancer biology, as well as into medications and treatment methods based on cancer hypoxia.

Methods

Ethics statement

This human subject research was approved by the National Cancer Center Hospital East Institutional Review Board (K23-2). A written informed consent was obtained from each patient. Animal experiments were approved by the Animal Ethics Committee of the National Cancer Center Hospital East (K13-015). We used horse blood, which was purchased from Nippon Bio-test Laboratories Inc., in the phantom experiment. The animal work that produced the blood samples was approved by the Animal Ethics Committee of the Nippon Bio-test Laboratories Inc.

Laser endoscope system

We developed a prototype laser endoscope system composed of two types of laser and a white fluorescent pigment body (20 mW, 473 nm laser diode, and 1 W, 445 nm blue laser diode; Nichia, Japan) as light sources and a commercial endoscope system (EG-590ZW gastroscope, and EC-590ZW3 colonoscope; Fujifilm, Japan).

Phantom

We created a vessel phantom composed of a glass microcapillary, Intralipid-10% (fat emulsion) and blood (horse blood, stored in an equal volume of Alsever's solution), inside a container of dimensions 60 mm×30 mm×30 mm (Fig. 2A). The vessel phantom imitates typical human tissue at a 100× magnified scale. The inside diameter of the glass microcapillary is 2 mm. The depth of glass microcapillary from the liquid surface is 5 mm. Thus, the vessel phantom imitates the 20-μm diameter vessel in human tissue at 50 μm depth. The size of the vessel is 100× magnified; therefore the scattering coefficient of Intralipid and absorption coefficient of blood is one hundredth that of typical human tissues. Blood is diluted with pure water so that the hematocrit value is 0.5%, 0.4% or 0.3%. Sodium hydrosulphite ($Na_2O_4S_2$) is used for de-oxygenation of blood. Transmittance spectra are measured with a spectral radiometer (TOPCON SR-UL1) and a Xenon light source, and the true value of oxygen saturation is calculated from transmittance spectra.

Dorsal skin-fold chamber mouse model

We anesthetized each mouse by intraperitoneal injection of 0.4 ml avertin (1.2 wt% 2,2,2-tribromoethanol and 1 wt% 2-propanol dissolved in saline). This treatment maintained the mouse under anethesia for about 30 min. To minimize pain, the following operation of mounting a window chamber was conducted within 15 min. We peeled a small part of the dorsal skin and then attached a custom-made skin-fold window chamber that kept the subcutaneous blood vessels in the skin-peeled area observable. The circular glass window was 9 mm in diameter. We prepared a suspension of A549 human lung cancer cells by mixing 2×10^5 cells with 40 μl of BD Matrigel™ and injected it under the

skin in the chamber. After the experiment, all the mice were sacrificed by deep euthanasia using diethyl ether.

Cell culture

A549 human lung cancer cells (ATCC) were cultured in Dulbecco's modified Eagle medium (DMEM) at 37°C.

In vivo imaging of alimentary tracts with pigs

We used two conventional female Large White and Duroc pigs (40 kg) bred in a closed colony. All efforts were made to minimize animal suffering. We anesthetized the pigs by firstly administration of 20 ml ketalar (500 mg/10 ml) intramuscularly and 250 mg isozol intravenously, and then inhalation of sevoflurane after intubation. Anesthesia was maintained via a circular breathing system. All the following procedures were carried out under the anesthesia. Under X-ray guidance with a fluoroscopic system (Powermobile C-ARM Angiographic System; Siemens), an angiographic catheter (Selecon safe tip; Terumo, Japan) was placed into the common hepatic artery, and a microcatheter (Progreat alpha; Terumo) was placed into the left gastroepiploic artery. We used Histacryl (B. Braun Biosurgicals) diluted 10-fold with Lipiodol (Terumo) as the embolic agent. We injected the agent with the micro catheter to embolize the arteries connected to the stomach. This embolization made the stomach partially hypoxic. The StO_2 map of the stomach was observed with the hemoglobin oxygen saturation imaging system. After the observation of the stomach, we opened the abdomen and removed the stomach for a histological evaluation. We also placed the endoscope at the esophagus and observed the change of the pig's oxygenation state before the stomach observation, after the stomach removal and after an intravenous administration of potassium chloride (KCl) to cause cardiac arrest.

Human subject research

Patients who had been confirmed to have pharyngeal, oesophageal, gastric, or colorectal neoplasia by previous endoscopic examination were enrolled. Eligibility criteria were as follows: age of 20 years or more; and male or female patients. After conventional endoscopy was performed, hypoxia imaging was observed using prototype endoscopy. To compare histologic findings to hypoxia imaging, all patients received endoscopic treatment, such as polypectomy, EMR or ESD after conventional and hypoxia imaging endoscopy. When comparing pathological findings, we determined the corresponding areas of neoplasia and non-neoplasia in the endoscope images and obtained StO_2 levels from the StO_2 map.

Pathological assessment

We performed immunohistochemical expression of HIF-1 alpha, which accumulates under hypoxia[5], to evaluate hypoxic status on the histological slide. Sections (5 μm) from paraffin-embedded slices that included the most representative area were selected and used for immunohistochemical staining of HIF-1 alpha (Rabbit polyclonal antibody to HIF-1 alpha(ab104072); Abcam, Tokyo, Japan). Citrate buffer (pH 6.0) was used for antigen retrieval, and antigen dilution was ×100. Human lung adenocarcinoma and squamous cell carcinoma were used as positive controls.

Statistical analysis

StO_2 levels were measured in both neoplastic and non-neoplastic areas for each patient. Stratified by cancer region, this paired data was compared using Wilcoxon signed-rank test. Among gastric cancer patients, we summarised the patient characteristics according to the remainder calculated by subtracting StO_2 levels of the normal tissue from those of tumor tissue, as in some cases, tumor tissue appeared as non-blue color (same color as normal tissues). All P values were two-sided.

Supporting Information

Video S1 Endoscopic video image showing the hypoxic feature of a colorectal adenoma in real time: white light image (left upper), pseudocolor StO_2 map (left lower) and overlayed image (right).
(ZIP)

Acknowledgments

We acknowledge the contributions of S. Tominaga (phantom experiment), T. Kobayashi, M. Satake, T. Kimura, M. Kobayashi, C. Yamauchi and Y. Shiraishi (*in vivo* imaging experiment), and H. Hasegawa (human subject research).

Author Contributions

Conceived and designed the experiments: KK HY AS HE AO. Performed the experiments: KK HY TS TY YO HI MK. Analyzed the data: HY TS SN. Contributed reagents/materials/analysis tools: TS SN. Contributed to the writing of the manuscript: KK HY.

References

1. Bertout JA, Patel SA, Simon MC (2008) The impact of O2 availability on human cancer. Nature Rev. Cancer 8: 967–975.
2. Hockel M, Schlenger K, Aral B, Mitze M, Schaffer U, et al. (1996) Association between tumour hypoxia and malignant progression in advanced cancer of the uterine cervix. Cancer Res. 56: 4509–4515.
3. Hanahan D, Weinberg RA (2011) Hallmarks of cancer: the next generation. Cell 144: 646–674.
4. Semenza GL (2003) Targeting HIF-1 for cancer therapy. Nature Rev. Cancer 3: 721–732.
5. Semenza GL (2008) Hypoxia-inducible factor 1 and cancer pathogenesis. IUBMB Life 60: 591–597.
6. Pennacchietti S, Michieli P, Galluzzo M, Mazzone M, Giordano S, et al. (2003) Hypoxia promotes invasive growth by transcriptional activation of the met protooncogene. Cancer Cell. 3: 347–361.
7. Sutherland RM (1998) Tumour hypoxia and gene expression—implications for malignant progression and therapy. Acta Oncol. 37: 567–574.
8. Keith B, Simon MC (2007) Hypoxia-inducible factors, stem cells, and cancer. Cell 129: 465–472.
9. Jordan BF, Runquist M, Raghunand N, Baker A, Williams R, et al. (2005) Dynamic contrast-enhanced and diffusion MRI show rapid and dramatic changes in tumour microenvironment in response to inhibition of HIF-1 alpha using PX-478. Neoplasia 5: 475–485.
10. Goh V, Engledow A, Rodriguez-Justo M, Shastry M, Peck J, et al. (2012) The flow-metabolic phenotype of primary colorectal cancer: assessment by integrated 18F-FDG PET/perfusion CT with histopathologic correlation. J. Nucl. Med. 53(5): 687–692.
11. Chitneni SK, Palmer GM, Zalutsky MR, Dewhirst MW (2011) Molecular Imaging of Hypoxia, J. Nucl. Med. 52: 165–168.
12. Zhang G, Palmer GM, Dewhirst MW, Fraser CL (2009) A dual-emissive-materials design concept enables tumour hypoxia imaging. Nature Materials 8: 747–751.
13. Harada H, Kizaka-Kondoh S, Hiraoka M (2005) Optical imaging of tumour hypoxia and evaluation of efficacy of a hypoxia-targeting drug in living animals. Mol. Imaging 4: 182–193.
14. Benaron DA, Parachikov IH, Friedland S, Soetikno R, Brock-Utne J, et al. (2004) Continuous, noninvasive, and localized microvascular tissue oximetry using visible light spectroscopy. Anesthesiology 100: 1469–1475.
15. Maxim PG, Carson JJ, Benaron DA, Loo BW Jr, Xing L, et al. (2005) Optical detection of tumours in vivo by visible light tissue oximetry. Technol. Cancer Res. Treat. 4: 227–234.
16. Sorg BS, Moeller BJ, Donovan O, Cao Y, Dewhirst MW (2005) Hyperspectral imaging of hemoglobin saturation in tumour microvasculature and tumour hypoxia development. J. Biomed. Opt. 10: 4400–4404.

17. Moy AJ, White SM, Indrawan ES, Lotfi J, Nudelman MJ, et al. (2011) Wide-field functional imaging of blood flow and hemoglobin oxygen saturation in the rodent dorsal window chamber. Microvasc Res. 82(3): 199–209.
18. Barkun JS, Aronson JK, Feldman LS, Maddern GJ, Strasberg SM, et al. (2009) Evaluation and stages of surgical innovations. Lancet 374: 1089–1096.
19. Brown JM, Wilson WR (2004) Exploiting tumour hypoxia in cancer treatment. Nature Rev. Cancer 4: 437–447.

ORIGINAL CONTRIBUTION

Clinical Impact of Elastic Laminal Invasion in Colon Cancer: Elastic Laminal Invasion-Positive Stage II Colon Cancer Is a High-Risk Equivalent to Stage III

Mitsuru Yokota, M.D.[1] • Motohiro Kojima, M.D.[2] • Shogo Nomura, M.Sc.[3]
Yusuke Nishizawa, M.D.[1] • Akihiro Kobayashi, M.D.[1] • Masaaki Ito, M.D.[1]
Atsushi Ochiai, M.D.[2] • Norio Saito, M.D.[1]

1 Division of Colorectal Surgery, National Cancer Center Hospital East, Kashiwa, Chiba, Japan
2 Division of Pathology, Research Center for Innovative Oncology, National Cancer Center Hospital East, Kashiwa, Chiba, Japan
3 Clinical Trial Section, Research Center for Innovative Oncology, National Cancer Center Hospital East, Kashiwa, Chiba, Japan

BACKGROUND: Elastic laminal invasion is defined as tumor invasion beyond the peritoneal elastic lamina. It is one of the factors affecting the prognosis of patients with colon cancer.

OBJECTIVE: This study aimed to investigate the clinical impact of elastic laminal invasion in colon cancer and the magnitude of the worse prognosis of elastic laminal invasion-positive, node-negative patients.

DESIGN: This was a retrospective cohort study.

SETTINGS: This study reviewed data from a tertiary care cancer center in Japan.

PATIENTS: The records of 436 patients with pT3 or pT4a colon cancer who underwent curative resection between January 1996 and December 2006 were reviewed.

MAIN OUTCOME MEASURES: The primary outcome measure was recurrence-free survival. Cox regression analyses established the factors associated with recurrence-free survival. Six groups formed by combining the factors were compared.

RESULTS: Of the patients with pT3 disease, those who were positive for elastic laminal invasion had a 5-year recurrence-free survival rate of 73.8% compared with a rate of 85.0% in those who were negative for elastic laminal invasion and 53.5% in patients with pT4 disease. Three unfavorable prognostic factors were identified, including lymph node metastasis, positive elastic laminal invasion, and a lack of adjuvant chemotherapy. Log-rank analysis revealed statistically significant differences in recurrence-free survival between group 1 (node negative, elastic laminal invasion negative, and no adjuvant chemotherapy) and group 3 (node negative, elastic laminal invasion positive, and no adjuvant chemotherapy). The HR for group 1 compared with group 3 was 0.49 (95% CI, 0.27–0.90). Furthermore, the HRs for group 2 (node positive, elastic laminal invasion negative, and received adjuvant chemotherapy) and group 4 (node positive, elastic laminal invasion positive, and received adjuvant chemotherapy) vs group 3 were 0.77 (95% CI, 0.35–1.69) and 1.36 (95% CI, 0.62–2.98).

LIMITATIONS: Our study has limited prediction accuracy of our prognostic stratification, and an analysis of small subgroups may not have been capable of detecting significant differences. In addition, a wide range of hematoxylin and eosin- and elastica-stained slides were examined per case.

CONCLUSIONS: Elastic laminal invasion adversely influences prognosis in pT3 and pT4a colon cancer. Although elastic laminal invasion positivity does not affect prognosis in node-positive patients receiving adjuvant chemotherapy, node-negative patients with elastic laminal invasion have a similar risk of recurrence as node-positive patients.

Funding/Support: Grant support for this study was provided by a National Cancer Center Research and Development Fund (23-A-14).

Financial Disclosure: None reported.

Presented at the Digestive Disease Week conference, Orlando, FL, May 18 to 21, 2013.

Correspondence: Norio Saito, M.D., Division of Colorectal Surgery, National Cancer Center Hospital East, 6-5-1 Kashiwanoha, Kashiwa, Chiba 277–8577, Japan. E-mail: norsaito@east.ncc.go.jp

Dis Colon Rectum 2014; 57: 830–838
DOI: 10.1097/DCR.0000000000000124

KEY WORDS: Colon cancer; Elastic laminal invasion; High-risk stage II; Serosal invasion.

In 2008, 1.2 million people received a new diagnosis of colorectal carcinoma (CRC), and 608,700 patients died of the disease, making it the fourth most common cause of cancer death globally.[1] However, in the United States and Europe, it is the second leading cause of cancer death.[2,3] In Japan, CRC is diagnosed in ≈105,000 patients each year and accounts for 42,000 deaths, making it the third leading cause of death from cancer.[4]

CRC is staged using the TNM system of the International Union Against Cancer (UICC),[5] in which primary tumor extension (T), regional lymph node involvement (N), and the presence of distant metastasis (M) are established to guide treatment and predict prognosis. Pathologic (p) T categories are divided into pT1 to pT4: pT3 disease is defined by subserosal tumor invasion and accounts for approximately half of all cases of CRC. The prognosis of patients with pT3 disease varies, which may be explained by differences in the depth of tumor invasion.[6–8] Nevertheless, although it has been suggested that pT3 disease be subclassified, it currently remains 1 category.

The peritoneal elastic lamina (PEL) is a component of the normal intestinal wall and can be identified histologically by elastica staining. It is situated beneath the visceral peritoneum and covers the intestinal wall. Subclassifying pT3 tumors according to their relationship with the PEL has been suggested as another method of pT3 classification. Patients with tumor invasion beyond the PEL are classified as having elastic laminal invasion (ELI).[9] Furthermore, the elastic lamina is used as a landmark of invasion of the visceral pleura in the TNM classification of lung cancer.[5] These facts guide us to focus on the PEL as a landmark of the classification of tumor spread.

Our previous study of 564 patients with stage II to IV CRC suggested that ELI was one of the factors affecting the prognosis of patients with colon cancer (CC) and an independent risk factor for tumor recurrence only among CC patients with stage II disease.[10] However, it is not yet clear that ELI status can be a prognostic factor under comprehensive analysis, including factors such as lymph node involvement and adjuvant chemotherapy.

The aim of this study was to investigate the clinical impact of ELI in patients diagnosed with pT3 and pT4a CC and the magnitude of the worse prognosis of patients with ELI-positive, node-negative CC (NNCC).

MATERIALS AND METHODS

Patients Selection and Follow-up

Of the 1103 consecutive patients who underwent surgery for CC at the National Cancer Center Hospital East between January 1996 and December 2006, 721 patients had pT3 or pT4a disease. The following patients were excluded: 1) patients with multiple or metachronous CC, 2) patients simultaneously or previously diagnosed with an advanced tumor other than CC, 3) patients with distant metastasis, 4) patients who received neoadjuvant therapy, and 5) patients in whom resection was incomplete (R1 and R2). Completeness of resection was classified as R0 (negative gross and pathologic margins), R1 (negative gross and positive microscopic margins), and R2 (positive gross margins). R1 and R2 were defined as incomplete resection. After exclusions, the clinical records of 439 patients with pT3 and pT4a CC were retrospectively studied. We began routinely administering 5-fluorouracil–containing adjuvant chemotherapy for patients with stage III disease in 2003, and 3 patients with stage II CC were excluded because they had also received adjuvant chemotherapy. Each patient's prospectively collected demographic, staging, histopathology, and prognostic outcome data were recorded. All of the cases were reclassified based on the 7th edition of the UICC TNM staging system.[5] We did not categorize isolated tumor deposits as pN1c to avoid overestimating the prognosis of patients with stage III disease. Follow-up after surgery was composed of serum tumor marker measurement every 3 months and chest and abdominal CT every 6 months for the first 3 years, then every 6 months for the next 2 years, and annually for 2 additional years. All of the patients were followed from the date of surgery to the last contact (death or last follow-up) or until December 31, 2011. Recurrence was defined as distant metastasis, local recurrence, or peritoneal dissemination; the final diagnosis was made by imaging (CT, MRI, and/or positron emission tomography CT), cytologic analysis, or biopsy, if necessary.

Written, informed consent to tissue collection and use for research was obtained. Conduct of the study was approved by our local ethics committee (National Cancer Center Hospital, No. 2012-067).

Histopathologic Analysis

We used the same histopathologic protocol as our previous study.[10] The resected specimens were fixed in 10% formalin, and the entire tumor was cut into 5-mm sections. Representative slices were embedded in paraffin, cut into 3-μm sections, and stained with hematoxylin and eosin (H&E) and elastica stain to allow evaluation of serial sections for ELI status and lymphovascular invasion (Fig. 1). We used the modified resorcin-fuchsin method for the latter.[11] There is a defect of the PEL at the mesenteric attachment; therefore, we undertook elastica staining on at least 1 whole section where the tumor was closest to the peritoneal surface to confirm the continuity of the PEL. The median numbers of H&E- and elastica-stained sections were 6 (range, 2–20) and 4 (range, 2–16). We defined cases with tumor invasion beyond the PEL as ELI positive (Fig. 1C

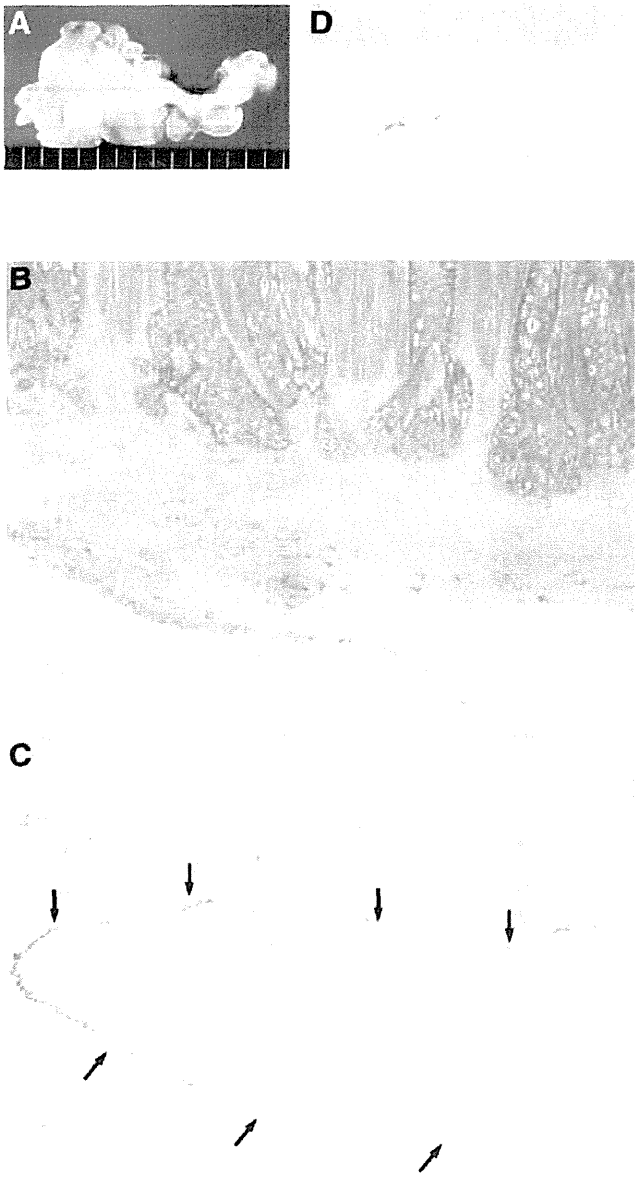

FIGURE 1. A, Cut surface of a tumor with elastic lamina invasion (ELI). Hematoxylin and eosin staining (B; ×40) and elastica staining (C; ×40; D, ×100) of the white box area in A. The peritoneal elastic lamina (PEL; arrows in C) is situated beneath the visceral peritoneum. C and D, Tumor invasion beyond the PEL represents ELI positivity.

and 1D). Continuity of the PEL in unaffected areas was confirmed regardless of the intensity of staining near the tumor. In cases with duplication of the PEL around the invasive front of the tumor, we determined cases with tumor invasion beyond the PEL to be ELI positive only when the PEL was judged the outermost layer of elastin. In cases in which the PEL had been disrupted, its estimated course was obtained by drawing a straight line between the residual PEL; only cases with invasion beyond the line were defined as ELI positive. ELI status was retrospectively evaluated by 2 pathologists blinded to the patient outcomes.

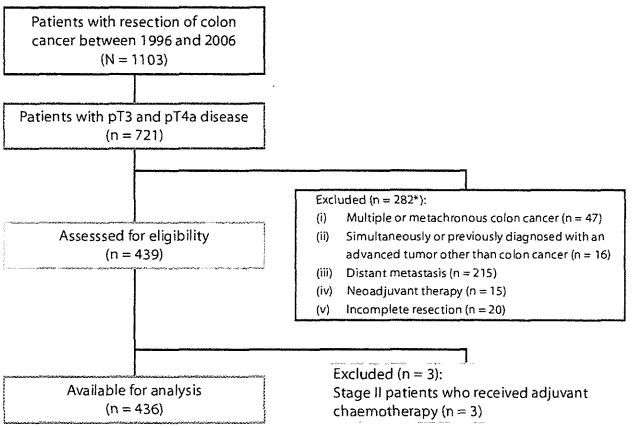

FIGURE 2. Consolidated Standards of Reporting Trials diagram of the study. *At least 1 of the criteria (i to v) was met.

Statistical Analysis

Our primary outcome measure was recurrence-free survival (RFS), defined as the time that elapsed between the date of surgery and any relapse or death from any cause. Overall survival (OS) was a secondary outcome, defined as the time from surgery to death from any cause. We chose RFS as the primary outcome to avoid the impact of treatments after recurrence on survival. Kaplan-Meier survival curves were plotted and compared using the log-rank test. Continuous variables were separated into 2 categories on the basis of their median values. All of the baseline characteristics were summarized as numbers and percentages.

To verify whether ELI status was an independent prognostic factor, we first performed multivariate Cox regression analyses for RFS. Baseline covariates included age (<65 or ≥65 years), sex (male or female), tumor size (<4.5 or ≥4.5 cm), histologic differentiation (well/moderately or poorly/mucinous), surgical technique (open or laparoscopic), lymphatic invasion (positive or negative), venous invasion (positive or negative), lymph node metastasis (positive or negative), number of lymph nodes retrieved (less than 12 or 12 or more), preoperative serum CEA level (<5 or ≥5 ng/mL), adjuvant chemotherapy (received or not received), and ELI (positive or negative).

The branch-and-bound algorithm of the Furnival and Wilson[12] variable selection procedure was applied to identify the risk factors using these candidate covariates. Next, we divided patients into all of the possible combinations based on the covariates identified in the Cox regression analyses so that their stratification would be meaningful. To establish the extent to which ELI adversely affected prognosis in NNCC, we compared the group consisting of patients with ELI-positive NNCC with groups composed of patients with node-positive CC (NPCC; stage III disease). We also applied the risk group to patients with pT3, because exclusion of patients with pT4a disease might have influenced our proposed risk stratification. Furthermore, we evaluated how the risk group affected OS.

TABLE 1. Patient characteristics and univariate analysis for RFS

	No. of patients (N = 436)		RFS	
Variable	*No.*	*%*	*5 y (%)*	*p[a]*
Age, y				
Median (range)	65.0 (26.0–92.0)			0.32
<65	208	47.7	76.2	
≥65	228	52.3	80.5	
Sex				
Male	251	57.6	76.1	0.17
Female	185	42.4	81.1	
Tumor location				
Right	146	33.5	83.7	0.08
Transverse	51	11.7	71.4	
Left	239	54.8	76.3	
Tumor stage				
pT3	393	90.1	81.0	<0.0001
pT4a	43	9.9	53.5	
Nodal status				
pN0	250	57.3	88.3	<0.0001
pN1	140	32.1	68.4	
pN2	46	10.6	54.8	
Tumor size, cm				
Median (range)	4.5 (0.6–16.5)			0.09
<4.5	196	45.0	75.0	
≥4.5	240	55.0	80.9	
Histologic differentiation				
Well/moderately	396	90.8	78.8	0.38
Poorly/mucinous	40	9.2	72.2	
Lymphatic invasion				
Negative	293	67.2	80.6	0.07
Positive	143	32.8	73.2	
Venous invasion				
Negative	102	23.4	89.0	0.002
Positive	334	76.6	74.9	
CEA, ng/mL				
Median (range)	3.9 (0.2–247.7)			0.27
<5	252	57.8	79.8	
≥5	184	42.2	76.0	
Type of surgery				
Open	267	61.2	78.0	0.84
Laparoscopic	169	38.8	78.6	
No. of lymph nodes retrieved				
Median (range)	26.5 (4.0–124.0)			0.58
<12	31	7.1	76.0	
≥12	405	92.9	78.4	
Adjuvant chemotherapy				
Received	71	16.3	78.4	0.98
Not received	365	83.7	77.2	
ELI				
Negative	254	58.3	85.1	<0.0001
Positive	182	41.7	68.8	

ELI = elastic laminal invasion; RFS = recurrence-free survival.
[a]*p* value was calculated by log-rank test (2 sided).

All of the statistical analyses were performed using SAS 9.3 (SAS Institute, Cary, NC). All *p* values were reported as 2 sided, and statistical significance was defined as values <0.05.

RESULTS

Patient Characteristics

A total of 436 patients with a median age of 65.0 years were enrolled (Fig. 2). Their characteristics were shown in Table 1. Tumors were located in the cecum in 26 patients (6.0%), the ascending colon in 120 (27.5%), the transverse colon in 51 (11.7%), the descending colon in 36 (8.3%), and the sigmoid colon in 203 (46.5%). Tumors were classified as stage IIA, IIB, IIIB, and IIIC in 236 (54.1%), 14 (3.2%), 165 (37.9%), and 21 patients (4.8%). Seventy-one patients (38.2%) with stage III CC received adjuvant chemotherapy after primary resection. Overall, 182 patients

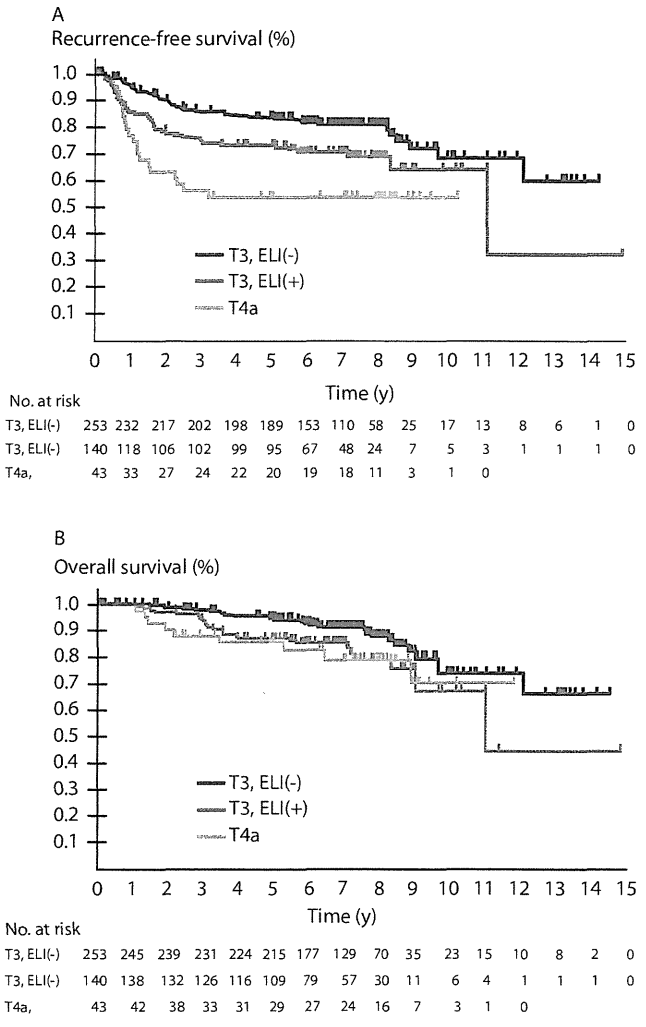

FIGURE 3. Kaplan-Meier curves depicting recurrence-free (A) and overall survival (B) based on the elastic laminal invasion status of 436 patients who underwent primary resection for colon cancer.

(41.7%) were identified as ELI positive, 140 (35.6%) of those with pT3 and 42 (97.7%) of those with pT4a disease.

Association Between ELI Status and Survival

The 5-year RFS and OS for all of the participants were 78.2% and 92.9%. The median follow-up was 7.1 years (range, 0.1–15.1 years). Of those who survived, 93.3% were followed for ≥3 years, and 88.0% were followed for ≥5 years. Tumor stage, nodal status, venous invasion, and ELI status influenced RFS (Table 1). Of the patients with pT3 disease, those who were ELI positive had a 5-year RFS of 73.8% compared with 85.0% for those who were ELI negative ($p = 0.002$) and 53.5% for patients with pT4 disease ($p = 0.02$; Fig. 3A). Tumors recurred in 95 (21.8%) of the 436 patients; the most common sites of recurrence were the liver (48 patients), lung (18 patients), and peritoneum (13 patients). The 5-year OS of ELI-positive patients with pT3 disease was 87.3% compared with 94.9% if ELI status was negative ($p = 0.02$) and 85.3% in patients with pT4 disease ($p = 0.82$; Fig. 3B). Overall, 63 patients died (14.4%): of those who died of CC, 28 were ELI positive and 14 were ELI negative; of those who died of other causes, 6 were ELI positive and 15 were ELI negative.

TABLE 2. Multivariate Cox regression analyses for RFS to assess the influence of risk factors

	RFS		
Variable	*HR*	*p*	*95% CI*
Lymph node metastasis (+)	2.96	<0.0001	1.95–4.49
Adjuvant chemotherapy (+)	0.50	0.01	0.29–0.85
ELI (+)	1.59	0.02	1.08–2.33

ELI = elastic laminal invasion; RFS = recurrence-free survival.

Multivariate Analyses

We performed Cox regression analyses on all 436 patients. For RFS, the branch-and-bound algorithm identified 3 unfavorable factors, including lymph node metastasis ($p < 0.0001$), lack of adjuvant chemotherapy ($p = 0.01$), and ELI positive status ($p = 0.02$; Table 2). Patients were divided into 6 groups based on these unfavorable factors, as shown in Table 3. We chose group 3 (node negative, ELI positive, and no adjuvant chemotherapy) as the reference value to compare with node-positive patients.

Evaluation of Prognosis

Kaplan-Meier curves for RFS in each group are shown in Figure 4A. The survival curves of group 5 (node positive, ELI negative, and no adjuvant chemotherapy) and group 6 (node positive, ELI positive, and no adjuvant chemotherapy) were almost identical ($p = 0.43$), and there was not a significant difference between group 2 (node positive, ELI negative, and received adjuvant chemotherapy) and group 4 (node positive, ELI positive, and received adjuvant chemotherapy; $p = 0.15$). There was, however, a significant difference between group 1 (node negative, ELI negative, and no adjuvant chemotherapy) and group 3 ($p = 0.001$). The RFS curve of group 3 lay between those of group 2 and group 4, both of which were composed of node-positive patients. The HR for group 1 vs group 3 was 0.49 (95% CI, 0.27–0.90), corresponding with a 51% relative reduction in the risk of recurrence. Furthermore, the HRs for groups 2 and 4 vs group 3 were 0.77 (95% CI, 0.35–1.69) and 1.36 (95% CI, 0.62–2.98).

When group 3 was compared with the other groups in terms of OS, similar trends were observed (Table 3 and Fig. 4B). The estimated OS Kaplan-Meier curve of group 3 was also between those of groups 2 and 4. The HRs for groups 2 and 4 vs group 3 were 0.88 (95% CI, 0.29–2.62) and 1.81 (95% CI, 0.61–5.41).

Findings After Exclusion of Patients With pT4a Disease

The impact of ELI status was reanalyzed using the same 6 groups after patients with pT4a disease were excluded

TABLE 3. Comparison of 5-year RFS and OS of the 6 stratified groups

Group		n	RFS		OS	
			5-y % (95% CI)	HR (95% CI)	5-y % (95% CI)	HR (95% CI)
1	N0,ELI(−),AC(−)	166	91.1 (85.4–94.6)	0.49 (0.27–0.90)	98.1 (94.2–99.4)	0.59 (0.25–1.41)
2	N1-2,ELI(−),AC(+)	42	83.0 (67.7–91.5)	0.77 (0.35–1.69)	97.6 (83.9–99.7)	0.88 (0.29–2.62)
3	N0,ELI(+),AC(−)	84	78.3 (67.8–85.7)	1.00	91.2 (82.4–95.7)	1.00
4	N1-2,ELI(+),AC(+)	29	69.0 (48.8–82.5)	1.36 (0.62–2.98)	89.7 (71.3–96.5)	1.81 (0.61–5.41)
5	N1-2,ELI(−),AC(−)	46	57.7 (41.9–70.6)	1.92 (1.03–3.57)	82.0 (67.1–90.5)	2.10 (0.88–5.01)
6	N1-2,ELI(+),AC(-)	69	55.9 (43.3–66.7)	2.36 (1.36–4.11)	79.5 (67.3–87.6)	2.64 (1.20–5.81)

N = nodal status; ELI = elastic laminal invasion; AC = adjuvant chemotherapy; RFS = recurrence-free survival; OS = overall survival.

(Table 4). The 5-year RFS for group 3 excluding those with pT4a disease (group 3′) was significantly worse than that for group 1′ (group 1 excluding those with pT4a disease; 81.1% vs 92.9%; $p = 0.003$). The RFS curve of group 3′ was similar to that of groups 2′ (group 2 excluding those with pT4a disease) and 4′ (group 4 excluding those with pT4a disease; group 3′ vs group 2′, $p = 0.61$; group 3′ vs group 4′, $p = 0.83$; Fig. 5A). The OS curve of group 3′ lay below that of groups 2′ and 4′ (group 3′ vs group 2′, $p = 0.41$; group 3′ vs group 4′, $p = 0.98$; Fig. 5B).

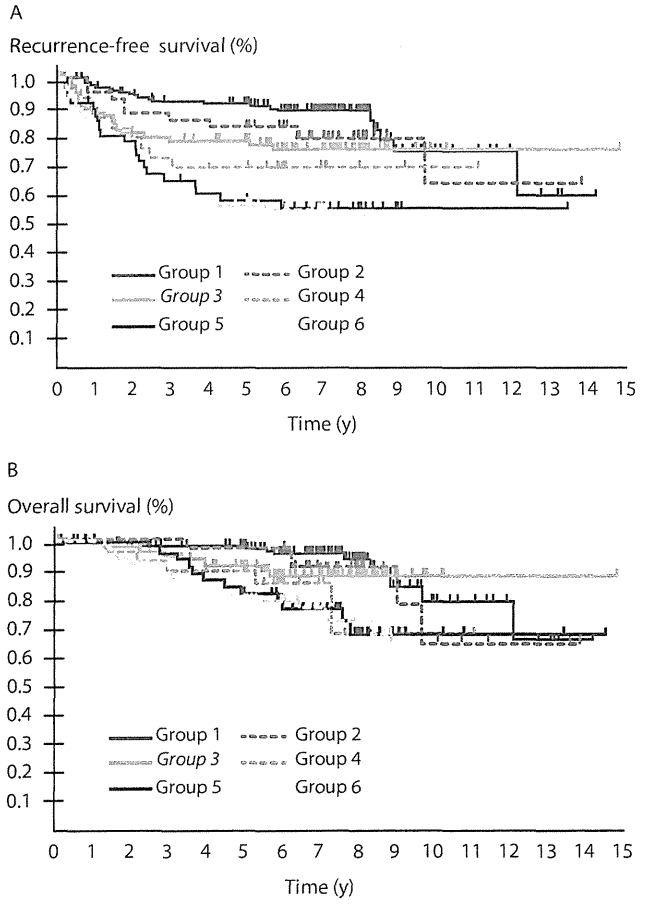

FIGURE 4. Kaplan-Meier curves depicting recurrence-free (A) and overall survival (B) of 6 groups of 436 patients who underwent primary resection for colon cancer, stratified according to elastic laminal invasion (ELI), lymph node metastasis, and adjuvant chemotherapy status. The green line represents group 3 (node negative, ELI positive, and no adjuvant chemotherapy).

DISCUSSION

ELI appears to influence outcome in patients with pT3 and pT4a CC. The RFS and OS of patients with ELI-negative NPCC (group 2) were better than those with ELI-positive NNCC (group 3). A similar trend was observed in previous reports based on the UICC 6th edition. Patients with stage IIIA (T1 to 2N1) disease had a better 5-year survival than those with stage IIA (T3N0) disease, and the Kaplan-Meier curve of patients with stage IIB (T4N0) disease lay approximately halfway between those of patients with stage IIIA and stage IIIB (T3-4N1) disease.[13,14] Whether the favorable outcome of patients with stage IIIA disease was because of limited tumor spread or adjuvant chemotherapy is unclear; these and our results show that some patients with stage II disease have a worse outcome than some with stage III disease.

Several studies have reported a variety of poor prognostic indicators in patients with stage II CC, including tumor necrosis,[15] perineural invasion,[15,16] male sex,[17] bowel obstruction,[17–19] tumor depth,[6,7,16–21] retrieval of less than 10 or 14 lymph nodes,[17,19] emergency presentation,[6] left colonic disease,[6] venous invasion,[20,21] lymphovascular invasion,[16,18,19,22] margin involvement,[20] differentiation pattern,[7] preoperative CEA level,[16] mucinous component of >50%,[18] tumor grade,[22] and tumor length.[22] Tumor depth and lymphovascular invasion have been identified most often. ELI status, which subdivides tumors invading beyond the muscularis propria, is also an indicator related to tumor depth. The "TNM Supplement: A Commentary on Uniform Use[23]" stated that the pT3 subclassification identified an extent of disease with a clinically relevant influence on outcome and could be used to determine the need for adjuvant chemotherapy.

There is a consensus that pT4 staging indicates a high risk of recurrence[24]; thus, the ELI status of patients other those with pT4a disease is also of great interest. The findings presented in Figure 5, from which patients with pT4a disease were excluded, show the poor prognosis of patients with ELI-positive NNCC with pT3 disease and indicate

TABLE 4. Comparison of 5-year RFS and OS of the 6 stratified groups excluding patients with pT4a disease

Group		n	RFS		OS	
			5-y % (95% CI)	HR (95% CI)	5-y % (95% CI)	HR (95% CI)
1′	N0,ELI(−),AC(−)	166	92.9 (88.9–97.0)	0.34 (0.16–0.73)	98.1 (95.9-NE)	0.46 (0.20–1.10)
2′	N1-2,ELI(−),AC(+)	41	82.6 (70.9–94.3)	0.79 (0.32–1.95)	97.5 (92.7-NE)	0.70 (0.23–2.09)
3′	N0,ELI(+),AC(−)	70	81.1 (71.9–90.4)	1.00	89.6 (82.3–96.9)	1.00
4′	N1-2,ELI(+),AC(+)	21	76.2 (58.0–94.4)	1.12 (0.40–3.12)	95.2 (86.1-NE)	0.81 (0.17–3.75)
5′	N1-2,ELI(−),AC(−)	46	59.8 (45.4–74.2)	2.09 (1.04–4.20)	82.0 (70.6–93.3)	1.65 (0.69–3.93)
6′	N1-2,ELI(+),AC(−)	49	62.5 (48.8–76.2)	2.21 (1.11–4.41)	80.1 (68.4–91.8)	2.04 (0.88–4.74)

N = nodal status; ELI = elastic laminal invasion; AC = adjuvant chemotherapy; RFS = recurrence-free survival; OS = overall survival; NE = not estimated.

that subclassification by ELI status allows valid conclusions to be made about outcome independent of tumor staging. The survival of patients with stage II CRC and pT3 deep tumor invasion (which represented tumors that had invaded beyond the PEL) has been reported to be equal to that of patients with stage II CRC and pT4 disease.[9] Therefore, a deeply invasive pT3 tumor, which fulfills the criteria for ELI used in this study, is a poor prognostic indicator.

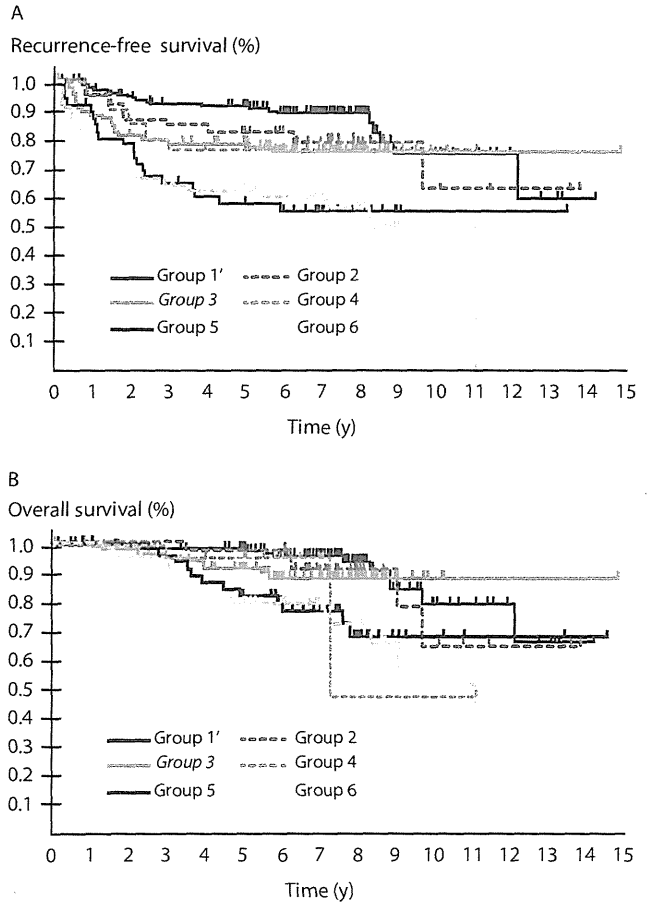

FIGURE 5. Kaplan-Meier curves depicting recurrence-free (A) and overall survival (B) of 6 groups of 393 patients who underwent primary resection for colon cancer, stratified according to elastic laminal invasion (ELI), lymph node metastasis, and adjuvant chemotherapy status after exclusion of those with pT4a disease. The green line represents group 3 excluding those with pT4a disease (group 3′; node negative, ELI positive, and no adjuvant chemotherapy).

Comparing the prognosis of stage II and III CC may help identify high-risk stage II patients. A small number of studies have reported the prognosis of stage II alongside that of stage III disease. The 5-year survival of patients with Dukes B CC determined to be at high risk by the Peterson index (43.3%) was worse than that of patients with Dukes C disease with a single lymph node metastasis (57.9%).[25] Patients with stage II CC and perineural invasion had significantly worse outcomes than stage III patients (5-year disease-free survival of 29% vs 56%; 5-year OS of 43% vs 67%).[26] This suggests that the Peterson index and perineural invasion may also be useful means of identifying a high-risk group for whom adjuvant chemotherapy might be recommended. Likewise, the RFS and OS of patients with ELI-positive NNCC were equivalent to those of patients with NPCC and pT3 or pT4a histology, corresponding with stage IIIB disease. Thus, ELI status appears to identify patients with high-risk stage II CC.

There is considerable variability in the incidence of serosal involvement in patients with Dukes stage B CC reported in previous studies,[27] which may reflect diagnostic difficulties.[28,29] One difficulty is that mesothelial cells are fragile, and the serosal surface may easily be disrupted during surgery and fixation. Another is that inflammatory and desmoplastic stromal reactions are often seen around the invasive tumor front. These problems can lead to underestimation of invasion because of the difficulty of demonstrating tumor cells on the peritoneal surface. In this regard, ELI may be advantageous because it is assessed from the inner surface of the serosa and is, therefore, not influenced by external trauma. Like vascular invasion, tumor spread might also be determined more objectively by routine elastica staining.[30,31]

ELI is sometimes affected by the tumor-associated inflammation around the invasive tumor front. In such cases, we speculate that the use of an estimated line and multiple histologic sections might provide a more precise and objective diagnosis. Nevertheless, we could not demonstrate ELI positivity in 2.3% of patients with pT4a disease. This is likely to be a consequence of marked in-

flammation at the tumor invasion front, making it impossible to determine ELI positivity in some patients with pT4a disease.

The prediction accuracy of our prognostic stratification is a limitation of our study, because we developed the risk group based only on the training set of 436 patients. A prospective study is needed to evaluate the validity and accuracy of our conclusions. Stratifying patients with CC into 6 groups based on 3 unfavorable factors led to an analysis of small subgroups that may not have been capable of detecting significant differences. Another limitation is that there was a wide range of H&E- and elastica-stained slides examined per case, because we did not adopt the protocol with a predefined the number of blocks and sections. This could cause bias in the ELI and pT4 rates.

The strength of our study was that not all of the patients with stage II CC routinely received adjuvant chemotherapy. If all of the patients predicted to have a poor outcome had received adjuvant chemotherapy, almost three quarters would have done so, making any comparison impossible.[32]

CONCLUSION

ELI status predicts prognosis in patients with pT3 and pT4a CC. Patients with ELI-positive NNCC have a worse outcome than those with ELI-negative histology and a prognosis similar to patients with stage III CC who received adjuvant chemotherapy. Therefore, although ELI positivity does not affect prognosis in patients with stage III CC receiving adjuvant chemotherapy, ELI is a strong prognostic factor to identify patients with high-risk stage II CC. Further prospective studies are needed to prove the reproducibility and validity of our findings.

REFERENCES

1. Jemal A, Bray F, Center MM, Ferlay J, Ward E, Forman D. Global cancer statistics. *CA Cancer J Clin.* 2011;61:69–90.
2. Siegel R, Naishadham D, Jemal A. Cancer statistics, 2012. *CA Cancer J Clin.* 2012;62:10–29.
3. Ferlay J, Parkin DM, Steliarova-Foucher E. Estimates of cancer incidence and mortality in Europe in 2008. *Eur J Cancer.* 2010;46:765–781.
4. Center for Cancer Control and Information Services, National Cancer Center, Japan. Latest cancer statistics. http://ganjoho.jp/public/statistics/pub/statistics01.html. Accessed November 20, 2012.
5. Sobin LH, Gospodarowicz MK, Wittekind C. *TNM Classification of Malignant Tumors.* 7th ed. West Sussex, United Kingdom: Wiley-Blackwell; 2009.
6. Merkel S, Wein A, Günther K, Papadopoulos T, Hohenberger W, Hermanek P. High-risk groups of patients with stage II colon carcinoma. *Cancer.* 2001;92:1435–1443.
7. Cianchi F, Messerini L, Comin CE, et al. Pathologic determinants of survival after resection of T3N0 (Stage IIA) colorectal cancer: proposal for a new prognostic model. *Dis Colon Rectum.* 2007;50:1332–1341.
8. Pollheimer MJ, Kornprat P, Pollheimer VS, et al. Clinical significance of pT sub-classification in surgical pathology of colorectal cancer. *Int J Colorectal Dis.* 2010;25:187–196.
9. Shinto E, Ueno H, Hashiguchi Y, et al. The subserosal elastic lamina: an anatomic landmark for stratifying pT3 colorectal cancer. *Dis Colon Rectum.* 2004;47:467–473.
10. Kojima M, Nakajima K, Ishii G, Saito N, Ochiai A. Peritoneal elastic laminal invasion of colorectal cancer: the diagnostic utility and clinicopathologic relationship. *Am J Surg Pathol.* 2010;34:1351–1360.
11. Puchtler H, Sweat F. Commercial resorcin-fuchsin as a stain for elastic fibers. *Stain Technol.* 1960;35:347–348.
12. Furnival GM, Wilson, R.W. Regression by leaps and bounds. *Technometrics.* 1974;16:499–511.
13. O'Connell JB, Maggard MA, Ko CY. Colon cancer survival rates with the new American Joint Committee on Cancer sixth edition staging. *J Natl Cancer Inst.* 2004;96:1420–1425.
14. Gunderson LL, Jessup JM, Sargent DJ, Greene FL, Stewart AK. Revised TN categorization for colon cancer based on national survival outcomes data. *J Clin Oncol.* 2010;28:264–271.
15. Mulcahy HE, Toner M, Patchett SE, Daly L, O'Donoghue DP. Identifying stage B colorectal cancer patients at high risk of tumor recurrence and death. *Dis Colon Rectum.* 1997;40:326–331.
16. Quah HM, Chou JF, Gonen M, et al. Identification of patients with high-risk stage II colon cancer for adjuvant therapy. *Dis Colon Rectum.* 2008;51:503–507.
17. Burdy G, Panis Y, Alves A, Nemeth J, Lavergne-Slove A, Valleur P. Identifying patients with T3-T4 node-negative colon cancer at high risk of recurrence. *Dis Colon Rectum.* 2001;44:1682–1688.
18. Lin CC, Lin JK, Chang SC, et al. Is adjuvant chemotherapy beneficial to high risk stage II colon cancer? Analysis in a single institute. *Int J Colorectal Dis.* 2009;24:665–676.
19. Koebrugge B, Vogelaar FJ, Lips DJ, et al. The number of high-risk factors is related to outcome in stage II colonic cancer patients. *Eur J Surg Oncol.* 2011;37:964–970.
20. Petersen VC, Baxter KJ, Love SB, Shepherd NA. Identification of objective pathological prognostic determinants and models of prognosis in Dukes' B colon cancer. *Gut.* 2002;51:65–69.
21. Morris M, Platell C, de Boer B, McCaul K, Iacopetta B. Population-based study of prognostic factors in stage II colonic cancer. *Br J Surg.* 2006;93:866–871.
22. Gertler R, Rosenberg R, Schuster T, Friess H. Defining a high-risk subgroup with colon cancer stages I and II for possible adjuvant therapy. *Eur J Cancer.* 2009;45:2992–2999.
23. Wittekind C, Compton CC, Brierley J. *TNM Supplement: A Commentary on Uniform Use.* 4th ed. West Sussex, United Kingdom: Wiley-Blackwell; 2012.
24. Shepherd NA, Baxter KJ, Love SB. The prognostic importance of peritoneal involvement in colonic cancer: a prospective evaluation. *Gastroenterology.* 1997;112:1096–1102.
25. Morris EJ, Maughan NJ, Forman D, Quirke P. Who to treat with adjuvant therapy in Dukes B/stage II colorectal cancer? The need for high quality pathology. *Gut.* 2007;56:1419–1425.
26. Liebig C, Ayala G, Wilks J, et al. Perineural invasion is an independent predictor of outcome in colorectal cancer. *J Clin Oncol.* 2009;27:5131–5137.

27. Stewart CJ, Morris M, de Boer B, Iacopetta B. Identification of serosal invasion and extramural venous invasion on review of Dukes' stage B colonic carcinomas and correlation with survival. *Histopathology.* 2007;51:372–378.
28. Kojima M, Yokota M, Saito N, Nomura S, Ochiai A. Elastic laminal invasion in colon cancer: diagnostic utility and histological features. *Front Oncol.* 2012;2:179.
29. Puppa G, Shepherd NA, Sheahan K, Stewart CJ. Peritoneal elastic lamina invasion in colorectal cancer: the answer to a controversial area of pathology? *Am J Surg Pathol.* 2011;35:465–468.
30. Kirsch R, Messenger DE, Riddell RH, et al. Venous invasion in colorectal cancer: impact of an elastin stain on detection and interobserver agreement among gastrointestinal and nongastrointestinal pathologists. *Am J Surg Pathol.* 2013;37:200–210.
31. Abdulkader M, Abdulla K, Rakha E, Kaye P. Routine elastic staining assists detection of vascular invasion in colorectal cancer. *Histopathology.* 2006;49:487–492.
32. O'Connor ES, Greenblatt DY, LoConte NK, et al. Adjuvant chemotherapy for stage II colon cancer with poor prognostic features. *J Clin Oncol.* 2011;29:3381–3388.

Pathology

Pathology International 2014; **64**: 209–216

doi:10.1111/pin.12164

Original Article

Optimal fixation for total preanalytic phase evaluation in pathology laboratories. A comprehensive study including immunohistochemistry, DNA, and mRNA assays

Masaaki Sato,[1] Motohiro Kojima,[1] Akiko Kawano Nagatsuma,[1] Yuka Nakamura,[1] Norio Saito[2] and Atsushi Ochiai[1]

[1]*Division of Pathology, Research Center for Innovative Oncology, National Cancer Center,* [2]*Colorectal and Pelvic Surgery Division, National Cancer Center Hospital East, Kashiwa, Chiba, Japan*

The purpose of this study was to set the optimal preanalytical fixation protocol to enhance analytical and postanalytical phase accuracy and consistency. Twenty-five normal colorectal tissues were fixed using various formalin concentrations, pHs, and fixation periods. All specimens were embedded in paraffin and 4 μm sections were used for immunohistochemistry of Ki-67, and extraction and amplification of DNA and RNA. The Ki-67 labeling index and the successful gene amplification rate for DNA and mRNA were evaluated and compared among variously fixed tissue samples. Ki-67 positivity was enhanced by low pH and short fixation time, and was influenced by the type of antibody, but not by the staining (with or without using an autostainer) method. DNA amplification by PCR was strongly influenced by pH of formalin. cDNA amplification could be accomplished only with the shortest PCR fragment of 142 bp, and longer fixation times impaired the amplification. These data suggest that multiple different factors influence immunohistochemical results and gene amplification using DNA and mRNA. We recommend, based on data from this comprehensive analysis, a 10% neutral buffered formalin and fixation times of no longer than 1 week to produce consistent immunohistochemical slides and DNA amplification within 500 bp in pathology laboratories.

Key words: fixation, pathology, preanalytic phase

The numerous components of laboratory test processes can be categorized into preanalytic, analytic, and postanalytic phases. Many laboratory tests using formalin-fixed and paraffin-embedded tissue samples in the preanalytic phase have been developed. Fixation is one of the most important steps in the preanalytic phase in pathological testing. Multiple factors including kinds of fixative, fixation duration, and acidity levels have been reported to have an effect on immunohistochemical results and gene amplification. For these reasons, a standardized and optimized fixation protocol for pathology laboratories would allow for more consistent and accurate data to be produced and enable better informed decisions based on the results.[1–8]

However, the current recommendations for preanalytic phase testing vary depending on what organ, therapy, or procedure (such as protein, DNA, or RNA assay) is being used.[9–18] Furthermore, most studies investigating the effects of fixation in laboratory testing have dealt with only one kind of laboratory test target. A standardized fixation protocol for pathology laboratories should be made available. We analyzed Ki-67 immunohistochemistry (IHC) testing and polymerase chain reaction (PCR)-based gene amplification using DNA and mRNA from one samples that was fixed by different protocols to clarify how variations in fixation influence postanalytic results in different assays. In regards to IHC testing, we also evaluated the effect of staining procedures, autostainer or manual staining, and different antibody clones, to search for the best way to reduce the effect of nonstandardized fixation protocols.

In this study, we performed comprehensive analyses using IHC and PCR procedures on one tissue block to develop an optimized fixation protocol available for use in pathology laboratories to enhance testing accuracy and consistency.

MATERIALS AND METHODS

Sample preparation

Twenty-five cases of the normal colorectal tissue samples 2.0 × 1.0 cm in size were obtained from surgically resected

Correspondence: Atsushi Ochiai, MD, PhD, Research Center for Innovative Oncology, National Cancer Center Hospital East, 6-3-1 Kashiwanoha, Kashiwa, Chiba, 277-8577, Japan. Email: aochiai@east.ncc.go.jp

Received 21 January 2014. Accepted for publication 2 April 2014.

Table 1 Types of fixatives

Fixatives	Buffer	pH value
10% NeuBF		7.5
10% NonBF	non	4.1
10% at pH 4	100 mM citrate	4.1
10% at pH 6	100 mM phosphate	6.1
10% at pH 7	100 mM phosphate	7.0
10% at pH 8	100 mM phosphate	7.9
20% NeuBF		7.5
20% NonBF	non	3.9

10% NeuBF, 10% neutral buffered formalin (Wako); 10% NonBF, 10% formalin; 10% at pH 4, 10% formalin with buffer at pH 4; 10% at pH 6, 10% formalin with buffer at pH 6; 10% at pH 7, 10% formalin with buffer at pH 7; 10% at pH 8, 10% formalin with buffer at pH 8; 20% NeuBF, 20% neutral buffered formalin (Wako); 20% NonBF, 20% formalin.

colorectal cancer cases at the National Cancer Center Hospital East between 2011 and 2012. All obtained tissues were fixed in 100 mL of formalin with various pHs and concentrations within 1 hour after removal from the colon. The eight types of formalin solutions are shown in Table 1. These specimens were fixed for 24 h, 48 h, 1 week, or 2 weeks. All differently fixed tissues were processed using Vacuum Rotary VRX-23 (Sakura Finetek, Tokyo, Japan), and embedded in paraffin. The present study was approved by the local research ethics committee of the National Cancer Center Hospital East (No.21–080).

Immunohistochemistry

The tissue was cut from paraffin blocks in 4 μm sections using a microtome and stretched on a water bath at 43°C, then mounted on glass slides. The slides were incubated at 37°C overnight. Ki-67 staining was performed manually by the standard immunohistochemical method. The slides were deparaffinized in xylene and hydrated in ethanol. Antigen retrieval was performed with 10 mM citrate buffer (pH 6.0) in a microwave oven at 95°C for 20 min. Endogenous peroxidase was blocked by incubation for 15 min with 0.3% hydrogen peroxidase in methanol. Nonspecific binding was blocked by incubating in phosphate-buffered saline (PBS) containing 2% normal swine serum and 0.1% sodium azide for 30 min. The primary antibody was diluted in PBS containing 2% normal swine serum and 0.1% sodium azide. The sections were incubated with mouse anti-human Ki-67 antibody with 1:100 dilutions for 1 h at room temperature. The clone MIB-1 (Dako, Glostrup, Denmark) monoclonal antibody against Ki-67 was used. After the wash with PBS, slides were incubated for 30 min using Dako Envision Labelled Polymer-HRP anti-mouse. The staining was visualized with 3,3′-diaminobenzidine for 4 min and counterstained with Mayer's hematoxylin, dehydrated in ethanol, and cleared in xylene. Other antigen retrieval methods were also performed using Target Retrieval Solution, pH 9 (Dako) or Dako Proteinase K, Ready-to-use (Dako).

Additionally, to evaluate the effect of different staining procedures, the staining for Ki-67 was carried out with a Dako Autostainer Link 48 (Dako) and a BenchMark Ultra (Ventana Medical Systems, Tucson, AZ) according to the manufacturer's instructions. The clone used in the autostainer was MIB-1 in Dako Autostainer Link 48, and it was 30-9 in BenchMark Ultra; the effect of the different clones was evaluated. Ki-67 stained slides were digitized using Hamamatsu NanoZoomer (Hamamatsu Photonics, Hamamatsu, Japan), and then Ki-67 positive nuclei were counted manually using the hot spot method.[19] High power ×40 field photos with 0.1 mm^2 field view were taken and all nuclei and Ki-67 positive nuclei were counted to evaluate Ki-67 positivity.

Nucleic acids extraction

Nucleic acids were extracted from 10 × 10 μm-thick sections for DNA and from 5 × 10 μm-thick sections for RNA using QIAamp DNA FFPE Tissue Kit (Qiagen, Tokyo, Japan) and RNeasy FFPE Kit (Qiagen), respectively.

PCR assays

DNA and RNA were assessed by PCR, and 1 μL of the sample was used as a PCR template. PCR was performed using the PrimeSTAR Max DNA Polymerase (Takara Bio, Shiga, Japan) according to the manufacturer's recommendations (thermal cycling conditions: 35 cycles of 98°C for 10 s, 55°C for 5 s, and 72°C for 5 s). RT-PCR was performed using the PrimeScript RT reagent Kit (Perfect Real Time) (Takara Bio, Shiga, Japan) for cDNA synthesis using random 6 mers according to the manufacturer's recommendations (thermal cycling conditions: 1 cycle of 37°C for 15 min and 85°C for 5 s). PCR amplification of ACTB (142 bp and 307 bp) and GAPDH (500 bp) were evaluated in genomic DNA. PCR amplification of GAPDH (142 bp) and TBP (161 bp, 252 bp, and 300 bp) were evaluated in cDNA. The 142 bp fragment of GAPDH and the 161 bp and 300 bp fragments of TBP span 1 intron, and the 252 bp fragment of TBP spans 2 intron sequences. The primer sequences are shown in Table S1.[20,21] Degraded DNA was evaluated using an Agilent 2100 Bioanalyzer (Agilent, Santa Clara, CA, USA).

Statistical analysis

To evaluate the effect of different type of formalin in the result of Ki-67 positivity, sections fixed with 10% NeuBF were used as a control, and the differences between the other types

were evaluated. To evaluate the effect of fixation time in the result of Ki-67 positivity, sections fixed for 24 h were used as a control, and sections fixed for 2 weeks were evaluated. To elucidate the effect of using an autostainer versus manual staining and of using different antibodies, manual staining was used as a control.

Student's *t*-test was used to determine statistically significance differences. The *P* value was set at 0.05.

RESULTS

Effect of pH and concentration of formalin in Ki-67 positivity

All sections under various fixation protocols showed nuclear expression in the basal crypt of epithelial cells in Ki-67 IHC. Figure 1 shows the Ki-67 positivity by fixation under different conditions such as various pHs, formalin concentrations, fixation times, and fixations by manual staining. Compared to the 10% NeuBF fixation, specimens fixed with the low pH formalin of pH 4 showed higher Ki-67 positivity in the 24 h and 48 h fixations. Ki-67 positivities in 10% NonBF for the 24 h and 48 h fixations, and in 10% formalin at pH 6 for the 48 h fixation, were significantly higher than that seen in 10% NeuBF ($P < 0.05$, Fig. 1a,b). The high pH formalin of pH 7 or pH 8 tended to show less Ki-67 positivity in the 1 week and 2 week fixations, but it was not statistically significant (Fig. 1c,d). Ki-67 positivity was not affected by 20% NeuBF and NonBF. Ki-67 positivity in all fixation protocols was low in the 2 week fixation when compared to the 1 week fixation. Furthermore, pH values of NonBF changed from 4 to 5 or 6 during the duration of the fixation (Fig. 1e,f).

Effect of fixation time in Ki-67 positivity

The effect of fixation time on Ki-67 positivity was evaluated under variable fixation times and using different staining procedures (Fig. 2). Ki-67 positivity was attenuated by longer fixation time, regardless of the difference in fixatives. Furthermore, this attenuation was notable after 1 or 2 week fixation (Fig. 2a). The same phenomenon was observed with either the manual or auto staining (Fig. 2b,c). And the same phenomenon was confirmed by using different antigen retrieval of pH 9 in manual staining. Sections treated with proteinase K for 3 min or 6 min were also performed, but positive stainings were not observed (Fig. 2d).

Effect of staining procedure

We evaluated the effect of the staining protocol between the manual and the autostaining system and also the effect of using different antibodies. Ki-67 positivity was compared between manual stained and Dako Autostainer Link 48 stained samples using the same MIB-1 antibody. Equivalent Ki-67 positivity was found between sections stained manually and with the Autostainer Link 48 (Fig. 3). In addition, regardless of the difference in the fixation protocol, similar Ki-67 positivity was observed between manual and Dako Autostainer Link 48 staining. The effect of different antibody clones on Ki-67 positivity was evaluated by using clones of MIB-1 (Dako) with manual staining and the Dako Autostainer Link 48, and by using 30-9 (Ventana) with the BenchMark Ultra. Ki-67 positivity was much higher in sections using 30-9 and stained by the BenchMark Ultra (Fig. 3). The same tendency was preserved with different fixation solutions. These results indicated that different clones also have an effect on Ki-67 positivity.

Figure 4 shows the immunohistochemical staining of the Ki-67 expressions with different fixatives and fixation periods. Ki-67 positivity and intensity of expression were different depending on the fixation protocols. The intensity of Ki-67 (MIB-1) expression in the section fixed by 10% NonBF was stronger than that seen in samples fixed by 10% NeuBF (Fig. 4a,b). Fixation for 24 h showed stronger intensity of Ki-67 (MIB-1) expression than that seen after 2 weeks of fixation (Fig. 4b,c). In addition, the intensity of clone 30-9 expression by BenchMark Ultra was stronger than that of MIB-1 and manual staining (Fig. 4a,d). These results show that not only positivity, but also the staining intensity, were influenced by the fixation protocol or staining procedure.

Effect of pH and concentration of formalin and fixation time on PCR assay

Genomic DNA and total RNA were extracted from blocks using the different fixation protocols. The results of PCR amplification of different fragment sizes are shown in Table 2. As for genomic DNA, the success rate of PCR assay was higher in 10% neutral or high pH formalin fixation than in low pH (pH 4.1) or 20% formalin fixation. In 10% NeuBF, 10% formalin at pH 7 or 8 fixations, PCR within 500 bp was successfully performed within 2 weeks of fixation time. In low pH and 20% formalin fixation, the success rate was lower depending on the fragment size and fixation time. As for the cDNA from mRNA, perfect amplification was observed only in short fragments within 252 bp. Fragments of 142 bp were successfully amplified within 48 h. The success rate was correlated with the small size of the fragment and short time of fixation. Figure 5 shows the degree of degradation of genomic DNA from NeuBF and NonBF under variable fixation times. Genomic DNA from NonBF increased low molecular weight smear depending on fixation times. Genomic DNA from 10% NeuBF was little affected by fixation times.

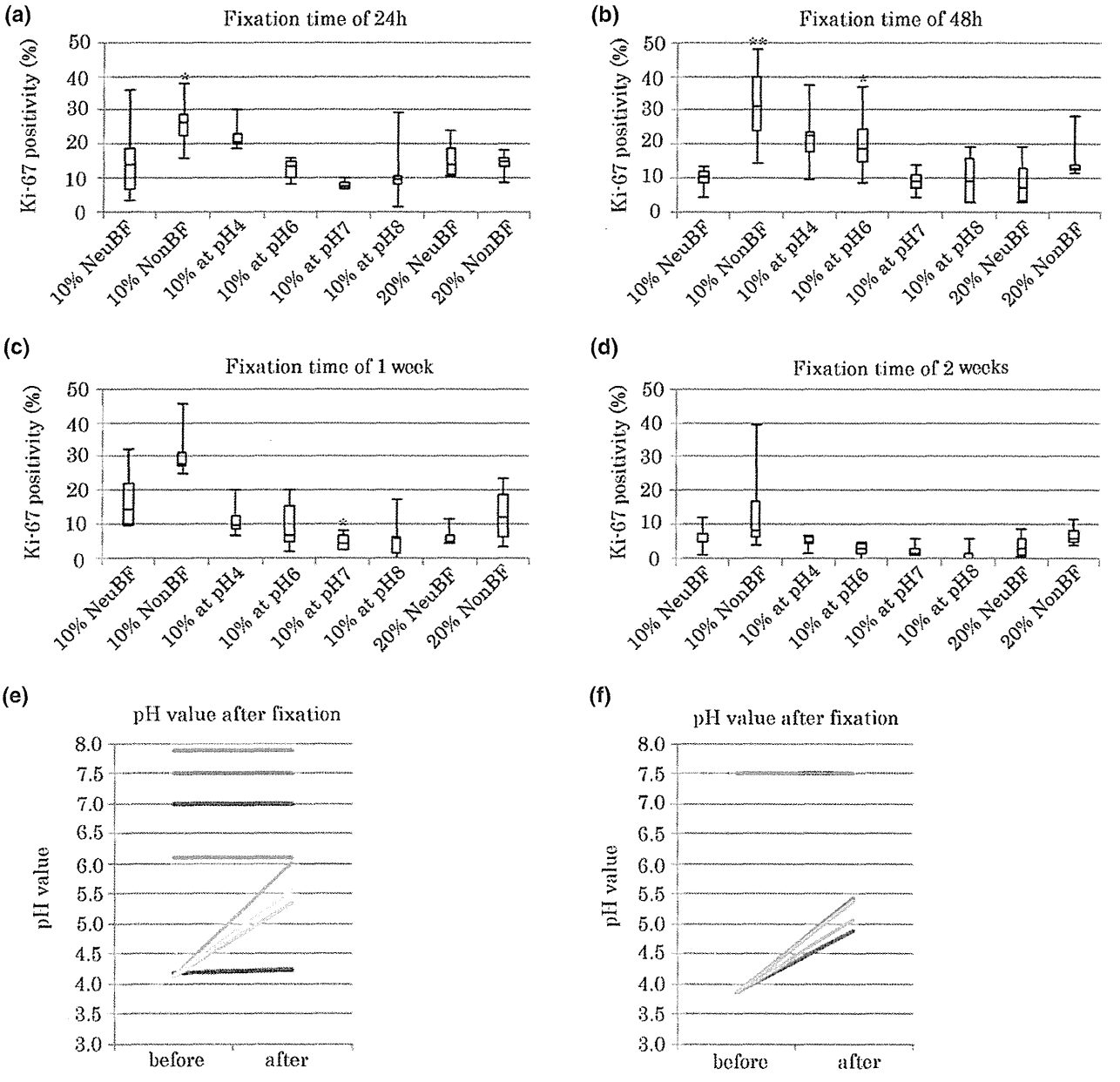

Figure 1 The effect of pH value and concentration in formalin with 24 h, 48 h, 1 week, and 2 week fixations by Ki-67 (MIB-1) manual staining. Box-and-whisker plots for comparison of the rate of Ki-67 positive nuclei stained manually in each fixative. Ki-67 (MIB-1) manually stained from specimens fixed (**a**) for 24 h, (**b**) for 48 h, (**c**) for 1 week, and (**d**) for 2 weeks. $^{*}P < 0.05$. $^{**}P < 0.01$. Change of pHvalue before and after fixation. (**e**) 10% NeuBF for 2 weeks; 10% with buffer at pH (4, 6, 7, and 8) for 2 weeks. 10% NonBF for 24 h, 48 h, 1 week and 2 weeks. (**f**) 20% NeuBF for 2 weeks; 20% NonBF for 24 h, 48 h, 1 week and 2 weeks. (**e**) —, 10% NeuBF 2w; —, 10% at pH4 2w; —, 10% at pH6 2w; —, 10% at pH7 2w; —, 10% at pH8 2w; —, 10% NonBF 24h; —, 10% NonBF 48h; —, 10% NonBF 1w; —, 10% NonBF 2w. (**f**) —, 20% NeuBF 2w; —, 20% NonBF 24h; —, 20% NonBF 48h; —, 20% NonBF 1w; —, 20% NonBF 2w.

DISCUSSION

Pathology laboratories are required to produce consistent data that are not affected by differences between laboratories. Recent progress in laboratory testing enables researchers to analyze not only protein expression but also DNA and mRNA assay from formalin fixed, paraffin-embedded tissue samples. Our study is the first to attempt to establish a standard fixation protocol suitable for multiple laboratory tests.

Ki-67 protein expression used in IHC has been utilized for multiple purposes including pathological diagnoses or therapeutic determinations in many types of cancers. Therefore,

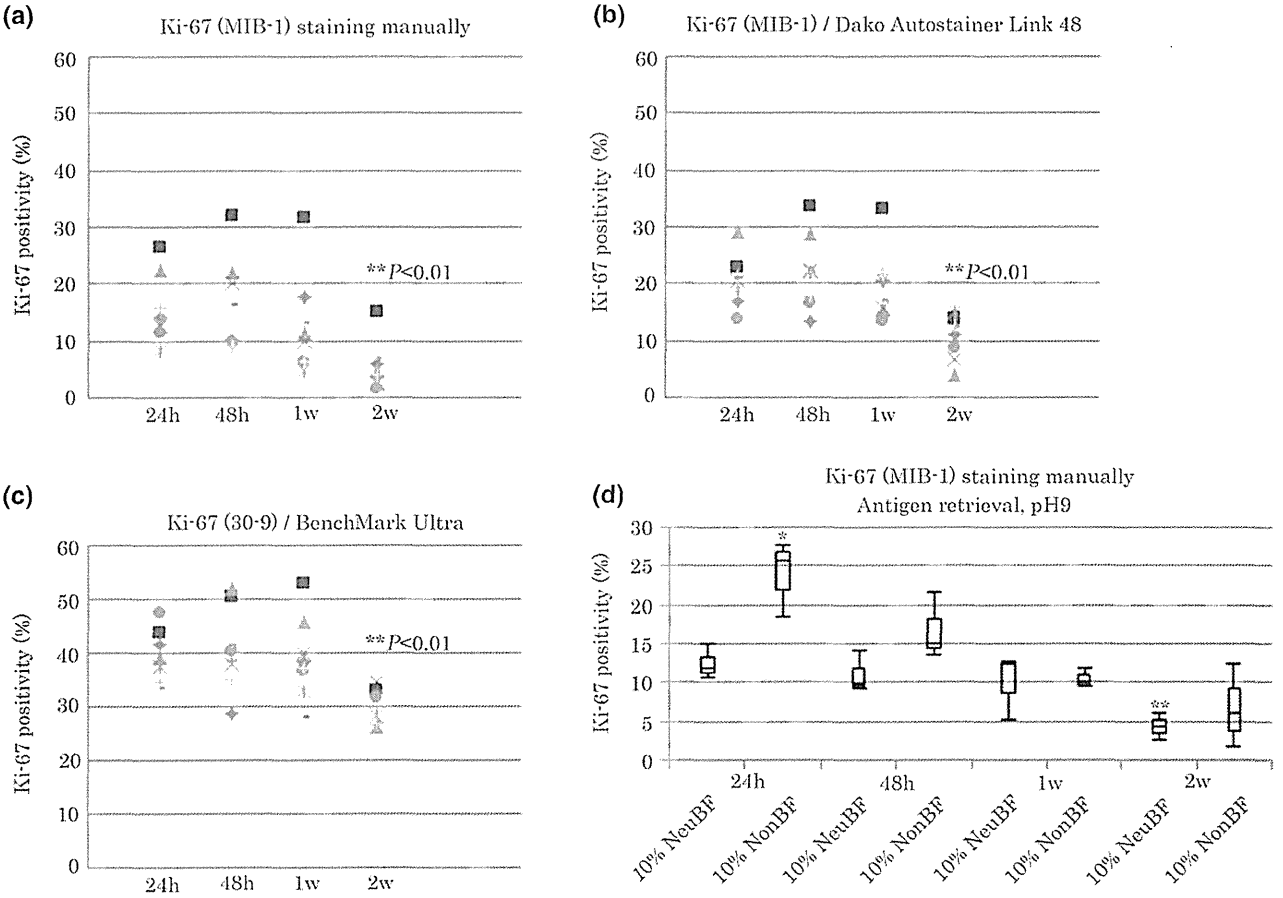

Figure 2 The effect of fixation time in Ki-67 (MIB-1) positivity using different staining procedures. Positive rate of (**a**) Ki-67 (MIB-1) staining manually, (**b**) Ki-67 (MIB-1) staining using Dako Autostainer Link 48, and (**c**) Ki-67 (30-9) staining using BenchMark Ultra with the change of fixaive time for each fixative. (**d**) The Ki-67 positivity by fixation under 10% NeuBF, 10%NonBF, various fixation times, and fixations by pH 9 antigen retrieval and manual staining. $^{*}P < 0.05$. $^{**}P < 0.01$. ◆, 10% NeuBF; ■, 10% NonBF; ▲, 10% at pH4; ✕, 10% at pH6; ✳, 10% at pH7; ●, 10% at pH8; ✚, 20% NeuBF; ▬, 20% NonBF.

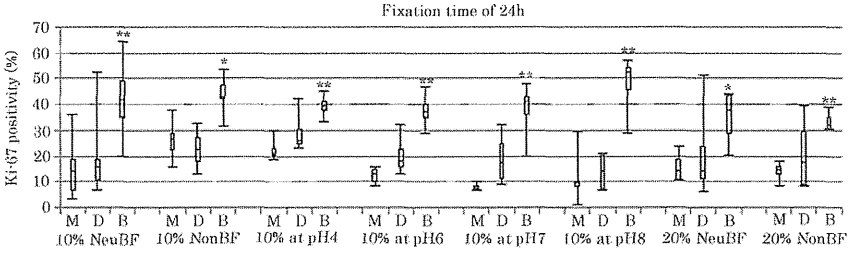

Figure 3 The effect of staining protocol using the autostaining system and different antibodies. Comparison of the positive rate of Ki-67 (MIB-1) staining manually (M), Ki-67 (MIB-1) staining using Dako Autostainer Link 48 (D) and Ki-67 (30-9) staining using BenchMark Ultra (B). $^{*}P < 0.05$. $^{**}P < 0.01$.

we selected the Ki-67 protein to study the effect of fixation protocols in protein assays. We evaluated the effect of acidity levels from pH 4 to pH 8, and Ki-67 positivity was strongly influenced by the pH level of the formalin. Furthermore, the pH value in non-buffered formalin changed during fixation. This result suggested that a neutral buffer is absolutely required to produce consistent data within different pathological laboratories, as reported in many recommendations.[2,11]

The concentration of formalin can also be one of the important factors to be managed in pathology laboratories.[22] However, compared with pH or fixation time, the effect of fixation was not as substantial, at least between 10% and 20% formalin solutions. As for the fixation times, although Ki-67 is reported to be robust across fixation times, our results show marked reduction in the protein expression between 1 to 2 week fixation, regardless of the different

Table 2 PCR results in genomic DNA and cDNA

	Fixation	PCR results in genomic DNA			PCR results in cDNA			
Fixative	time	*ACTB* 142bp	*ACTB* 307bp	*GAPDH* 500bp	*GAPDH* 142bp	*TBP* 161bp	*TBP* 252bp	*TBP* 300bp
10% NeuBF								
	24h	100% ($n = 9$)	100% ($n = 9$)	100% ($n = 9$)	100% ($n = 9$)	100% ($n = 9$)	100% ($n = 9$)	0% ($n = 9$)
	48h	100% ($n = 3$)	100% ($n = 3$)	100% ($n = 3$)	100% ($n = 3$)	66.6% ($n = 3$)	66.6% ($n = 3$)	0% ($n = 3$)
	1w	100% ($n = 3$)	100% ($n = 3$)	100%($n = 3$)	100% ($n = 3$)	33.3% ($n = 3$)	0% ($n = 3$)	0% ($n = 3$)
	2w	100% ($n = 3$)	100% ($n = 3$)	100% ($n = 3$)	100% ($n = 3$)	66.6% ($n = 3$)	33.3% ($n = 3$)	0% ($n = 3$)
10% NonBF								
	24h	100% ($n = 3$)	100% ($n = 3$)	100%($n = 3$)	100% ($n = 3$)	66.6% ($n = 3$)	66.6% ($n = 3$)	0% ($n = 3$)
	48h	100% ($n = 3$)	100% ($n = 3$)	100% ($n = 3$)	100% ($n = 3$)	100% ($n = 3$)	66.6% ($n = 3$)	0% ($n = 3$)
	1w	50% ($n = 4$)	75% ($n = 4$)	0% ($n = 4$)	100% ($n = 4$)	0% ($n = 4$)	0% ($n = 4$)	0% ($n = 4$)
	2w	0% ($n = 3$)	0% ($n = 3$)	0% ($n = 3$)	100% ($n = 3$)	0% ($n = 3$)	0% ($n = 3$)	0% ($n = 3$)
10% at pH 4								
	24h	66.6% ($n = 3$)	66.6% ($n = 3$)	66.6% ($n = 3$)	100% ($n = 3$)	100% ($n = 3$)	66.6% ($n = 3$)	0% ($n = 3$)
	48h	66.6% ($n = 3$)	100% ($n = 3$)	33.3% ($n = 3$)	100% ($n = 3$)	100% ($n = 3$)	33.3% ($n = 3$)	0% ($n = 3$)
	1w	0% ($n = 3$)	0% ($n = 3$)	0% ($n = 3$)	100% ($n = 3$)	0% ($n = 3$)	0% ($n = 3$)	0% ($n = 3$)
	2w	0% ($n = 3$)	0% ($n = 3$)	0% ($n = 3$)	33.3% ($n = 3$)	0% ($n = 3$)	0% ($n = 3$)	0% ($n = 3$)
10% at pH 6								
	24h	100% ($n = 3$)	100% ($n = 3$)	100% ($n = 3$)	100% ($n = 3$)	100% ($n = 3$)	100% ($n = 3$)	66.6% ($n = 3$)
	48h	66.6% ($n = 3$)	100% ($n = 3$)	100% ($n = 3$)	100% ($n = 3$)	100% ($n = 3$)	100% ($n = 3$)	0% ($n = 3$)
	1w	100% ($n = 3$)	100% ($n = 3$)	100% ($n = 3$)	100% ($n = 3$)	66.6% ($n = 3$)	0% ($n = 3$)	0% ($n = 3$)
	2w	100% ($n = 3$)	100% ($n = 3$)	0% ($n = 3$)	100% ($n = 3$)	33.3% ($n = 3$)	0% ($n = 3$)	0% ($n = 3$)
10% at pH 7								
	24h	100% ($n = 3$)	100% ($n = 3$)	100% ($n = 3$)	100% ($n = 3$)	100% ($n = 3$)	100% ($n = 3$)	0% ($n = 3$)
	48h	100% ($n = 3$)	100% ($n = 3$)	100% ($n = 3$)	100% ($n = 3$)	100% ($n = 3$)	100% ($n = 3$)	0% ($n = 3$)
	1w	100% ($n = 3$)	100% ($n = 3$)	100% ($n = 3$)	100% ($n = 3$)	100% ($n = 3$)	33.3% ($n = 3$)	0% ($n = 3$)
	2w	100% ($n = 3$)	100% ($n = 3$)	100% ($n = 3$)	66.6% ($n = 3$)	33.3% ($n = 3$)	33.3% ($n = 3$)	0% ($n = 3$)
10% at pH 8								
	24h	100% ($n = 3$)	100% ($n = 3$)	100% ($n = 3$)	100% ($n = 3$)	100% ($n = 3$)	100% ($n = 3$)	0% ($n = 3$)
	48h	100% ($n = 3$)	100% ($n = 3$)	100% ($n = 3$)	100% ($n = 3$)	66.6% ($n = 3$)	33.3% ($n = 3$)	0% ($n = 3$)
	1w	100% ($n = 3$)	100% ($n = 3$)	100% ($n = 3$)	100% ($n = 3$)	33.3% ($n = 3$)	0% ($n = 3$)	0% ($n = 3$)
	2w	100% ($n = 3$)	100% ($n = 3$)	100% ($n = 3$)	100% ($n = 3$)	33.3% ($n = 3$)	0% ($n = 3$)	0% ($n = 3$)
20% NeuBF								
	24h	100% ($n = 3$)	100% ($n = 3$)	100% ($n = 3$)	100% ($n = 3$)	100% ($n = 3$)	100% ($n = 3$)	0% ($n = 3$)
	48h	100% ($n = 3$)	100% ($n = 3$)	100% ($n = 3$)	100% ($n = 3$)	100% ($n = 3$)	100% ($n = 3$)	0% ($n = 3$)
	1w	100% ($n = 3$)	100% ($n = 3$)	100% ($n = 3$)	100% ($n = 3$)	33.3% ($n = 3$)	0% ($n = 3$)	0% ($n = 3$)
	2w	100% ($n = 3$)	100% ($n = 3$)	33.3% ($n = 3$)	100% ($n = 3$)	33.3% ($n = 3$)	33.3% ($n = 3$)	0% ($n = 3$)
20% NonBF								
	24h	100% ($n = 3$)	100% ($n = 3$)	100% ($n = 3$)	100% ($n = 3$)	66.6% ($n = 3$)	33.3% ($n = 3$)	0% ($n = 3$)
	48h	66.6% ($n = 3$)	33.3% ($n = 3$)	33.3% ($n = 3$)	100% ($n = 3$)	100% ($n = 3$)	100% ($n = 3$)	0% ($n = 3$)
	1w	66.6% ($n = 3$)	0% ($n = 3$)	0% ($n = 3$)	66.6% ($n = 3$)	33.3% ($n = 3$)	0% ($n = 3$)	0% ($n = 3$)
	2w	0% ($n = 3$)	0% ($n = 3$)	0% ($n = 3$)	33.3% ($n = 3$)	0% ($n = 3$)	0% ($n = 3$)	0% ($n = 3$)

ACTB, beta-actin; GAPDH, glyceraldehyde 3-phosphate dehydrogenase; TBP, TATA-binding protein.

fixatives or clones used.[23] Therefore, fixation times no longer than 1 week can be a practical standard for IHC. Use of an autostainer can provide stable IHC data, and the consistent data between autostaining and manual staining supports the routine utility of an autostainer after the establishment of a proper staining protocol. However, the clones must be chosen carefully because Ki-67 positivity was different between clones of MIB-1 and 30-9. In addition, fixation with low pH showed higher Ki-67 positivity, but may not produce a consistent result. Therefore, we must be aware that a protocol with higher Ki-67 positivity may not always be the best to produce consistent data.

In addition to the IHC, DNA and RNA assays are increasingly required to be performed on one sample embedded in paraffin. In those cases, stable PCR gene amplification is required in the analytical phase. It has been reported that acidic pH levels cause degradation of nucleic acids, and we also confirmed that the success rate of PCR gene amplification was lower in a pH 4 fixation.[24] As for genomic DNA, using 10% and 20% NeuBF, we consistently performed PCR assays of DNA amplification for those fragments shorter than or equal to 500 bp that had been fixed for between 24 h to 1 week. These data also support the use of NeuBF. As for cDNA from mRNA, the amplification was largely dependent on the length of the product size. However, the shortest fragment of 142 bp was successfully amplified after 1 week in NeuBF. These results also indicated it would be practical to use NeuBF solution and fixation times of between 24 h to 1

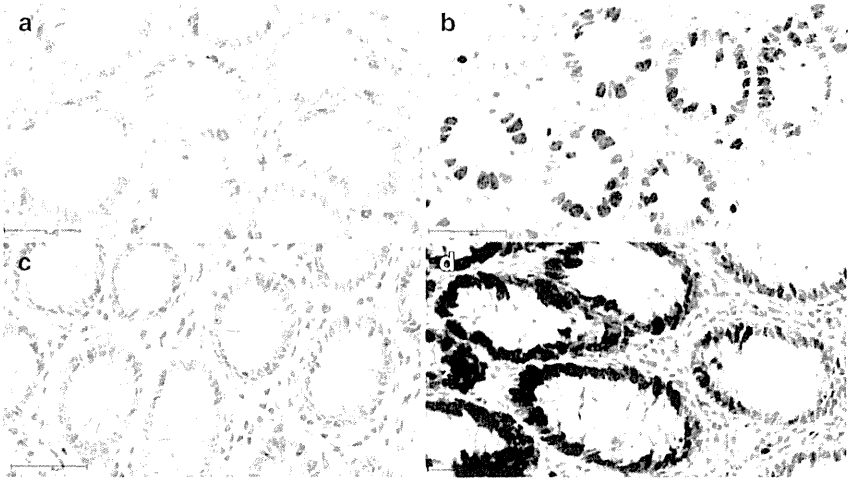

Figure 4 The immunohistochemical staining of Ki-67 expression with different fixatives and fixation periods. Ki-67 (MIB-1) staining manually (**a-c**), and Ki-67 (30-9) staining using BenchMark Ultra (**d**) of normal colonic mucosa according to the fixatives and fixation times. (**a, d**) 10% NeuBF for 24 h, (**b**) 10% NonBF for 24 h, (**c**) 10% with buffer at pH 4 for 2 weeks. Bar: 50 μm.

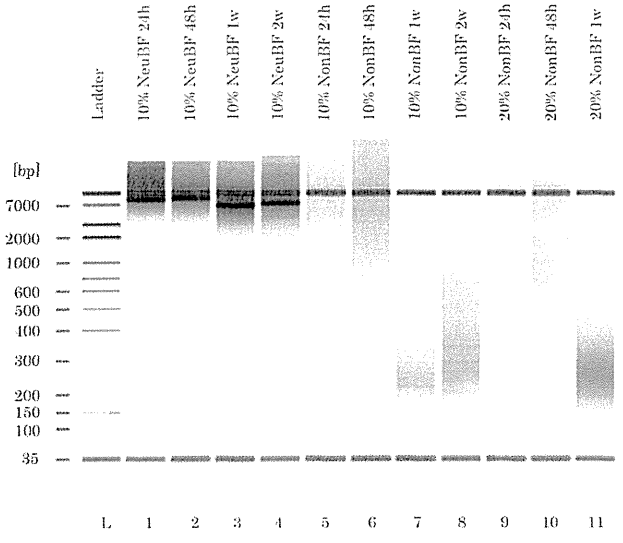

Figure 5 The degree of degradation of genomic DNA from NeuBF and NonBF under variable fixation times. L: Ladder; Lane 1: 10% NeuBF for 24 h; Lane 2: 10% NeuBF for 48 h; Lane 3: 10% NeuBF for 1 week; Lane 4: 10% NeuBF 2 weeks; Lane 5: 10% NonBF for 24 h; Lane 6: 10% NonBF for 48 h; Lane 7: 10% NonBF for 1 week; Lane 8: 10% NonBF for 2 weeks; Lane 9: 20% NonBF for 24 h; Lane 10: 20% NonBF for 48 h; Lane 11: 20% NonBF for 1 week.

week in the evaluation of DNA and RNA assays. Recently, alternative fixative with better preservation of nuclear acid than formaldehyde were reported.[25] Such a fixative may also be available when longer fragment analysis was required for the pathology laboratory in the future. On the other hand, at present, it is thought that NeuBF is a superior fixative for both protein and nucleic acids than NonBF.[26,27]

In conclusion, fixation protocols must be standardized to provide consistent result from multiple assays performed in different pathology laboratories. Taking these comprehensive results together, we recommend 10% NeuBF solution and fixation time of no longer than 1 week to obtain a uniform result in IHC, DNA, and RNA assays.

ACKNOWLEDGMENT

The authors thank Sachiko Fukuda for her excellent technical assistance. This study was supported in part by a Grant-in-Aid for Cancer Research (23-A-3) from the Ministry of Health, Labor and Welfare, Japan.

REFERENCES

1 Zarbo RJ. The oncologic pathology report. Quality by design. *Arch Pathol Lab Med* 2000; **124**: 1004–10.
2 Hammond ME, Hayes DF, Dowsett M *et al.* American Society of Clinical Oncology/College of American Pathologists guideline recommendations for immunohistochemical testing of estrogen and progesterone receptors in breast cancer (unabridged version). *Arch Pathol Lab Med* 2010; **134**: e48–72.
3 Matsuda Y, Fujii T, Suzuki T *et al.* Comparison of fixation methods for preservation of morphology, RNAs, and proteins from paraffin-embedded human cancer cell-implanted mouse models. *J Histochem Cytochem* 2011; **59**: 68–75.
4 Chung JY, Braunschweig T, Williams R *et al.* Factors in tissue handling and processing that impact RNA obtained from formalin-fixed, paraffin-embedded tissue. *J Histochem Cytochem* 2008; **56**: 1033–42.
5 Nykänen M, Kuopin T. Protein and gene expression of estrogen receptor alpha and nuclear morphology of two breast cancer cell lines after different fixation methods. *Exp Mol Pathol* 2010; **88**: 265–71.
6 DE Maezo AM, Fedor HH, Gage WR *et al.* Inadequate formalin fixation decreases reliability of p27 immunohistochemical staining: Probing optimal fixation time using high-density tissue microarrays. *Hum Pathol* 2002; **33**: 756–60.
7 Turashvili G, Yang W, McKinney S *et al.* Nucleic acid quantity and quality from paraffin blocks: Defining optimal fixation processing and DNA/RNA extraction techniques. *Exp Mol Pathol* 2012; **92**: 33–43.